METHODS TO IMPROVE UAV PERFORMANCE USING HYBRID-ELECTRIC ARCHITECTURES

Axel YEZEGUELIAN*
SAFRAN Landing Systems
FRANCE

axel.yezeguelian@safrangroup.com

Askin T. ISIKVEREN†
SAFRAN S.A.
AUSTRALIA

askin.isikveren@safrangroup.com

Keywords: Systems Architectures, Hybrid-Electric Propulsion, Organic Rankine Cycle, Integrated Vehicle Design, Aircraft Performance.

ABSTRACT

When comparing and contrasting different types of fixed-wing military aircraft on the basis of an energetic efficiency figure-of-merit, Unmanned Aerial Vehicles (UAVs) dedicated to tactical Medium Altitude Long Endurance (MALE) operations appear to have significant potential when Hybrid-Electric Propulsion and Power Systems (HEPPS) are implemented. Beginning with a baseline Eulair Drone, this investigation examined the feasibility of retro-fitting with an Autarkic-Parallel-HEPPS architecture in order to enhance performance of the original single diesel engine. In view of the low gravimetric specific energy performance attributes of batteries in the foreseeable future, the best approach was found to be one in which the Parallel-HEPPS architecture has the thermal engine augmented by an Organic Rankine Cycle (ORC). For this study, with the Outer Mould Lines fixed, the goal was to increase endurance without increasing the Eulair Drone Maximum Take-Off Weight beyond an upper limit of +10%. The intent was to also retain take-off distance and climb performance, or where possible improve upon these aspects. Therefore, since the focus of the work was on power scheduling, two primary control variables were identified as degree-of-hybridisation for useful power and cut-off altitude during the en route climb phase. Quasi-static methods were utilised for technical sub-space modelling and these modules were linked into a constrained optimisation algorithm. Results showed that an Autarkic-Parallel-HEPPS architecture comprising an ORC thermal energy recovery apparatus and high-end year-2020 battery, the endurance of the considered aircraft could be increased by 11%, i.e. a total of around 28 hours, including de-icing system, in-flight recharge, and emergency aircraft recovery capabilities. The same aircraft with the de-icing functionality removed resulted in a 20% increase in maximum endurance to 30 hours.

1 INTRODUCTION TO HYBRID-ELECTRIC ARCHITECTURES

In accordance with a published US convention (Committee on Propulsion and Energy Systems to Reduce Commercial Aviation Carbon Emissions, 2016) for aeronautical application Propulsion and Power Systems (PPS) that are electrified can be categorised broadly into three domains: (1) Hybrid-Electric; All-Electric; and, Turbo-Electric. Hybrid-Electric PPS (HEPPS) utilise thermal engines in combination with batteries. The batteries can either be exchanged during aircraft turn-around, or, recharged on-ground and/or in-flight via generators coupled to the thermal engine and/or through some form of energy recovery. It is highlighted to the

* Systems and Performance Simulation Engineer, Systems Equipment Division; formerly thesis student (Ecole Centrale Supélec, France) located at Energy and Propulsion Department, SAFRAN Tech.

† Senior Expert, Advanced Aircraft Concepts and Methods, Senior Group Expert, Integrated Aircraft Systems and Operation, Energy and Propulsion Department.

reader that apart from electro-chemical (Voltaic Piles such as batteries), other options for electrical energy storage include chemical (Grove Cells such as fuel cells) and electrical (capacitors). HEPPS architectures can be elaborated according to strategies arising out of series and parallel combinatorial arrangements. The distinctions are tied to the nature of the power node between each of the system constituents: in a series-hybrid arrangement, the node is electrical, whereas, in a parallel-hybrid, it is mechanical.

In the context of Tactical Medium-Altitude Long-Endurance (MALE) Unmanned Aerial Vehicles (UAVs) a set of candidates that constitutes a sufficiently expansive "concept cloud" of possible HEPPS architectures needs to be generated. Although not exhaustive, a total of eight propulsion system architectures, labelled as ARCH 0 through ARCH 7, are presented in this technical paper. Each can be found in Figure 1-1showing their respective schematic together with some brief remarks discussing the power-train approach, architecture functionality and operational capabilities. Down-selection of an architectural candidate needs to occur mindful of aircraft objectives and requirements, and this aspect is addressed later in the technical paper focusing on a worked Tactical MALE UAV example.

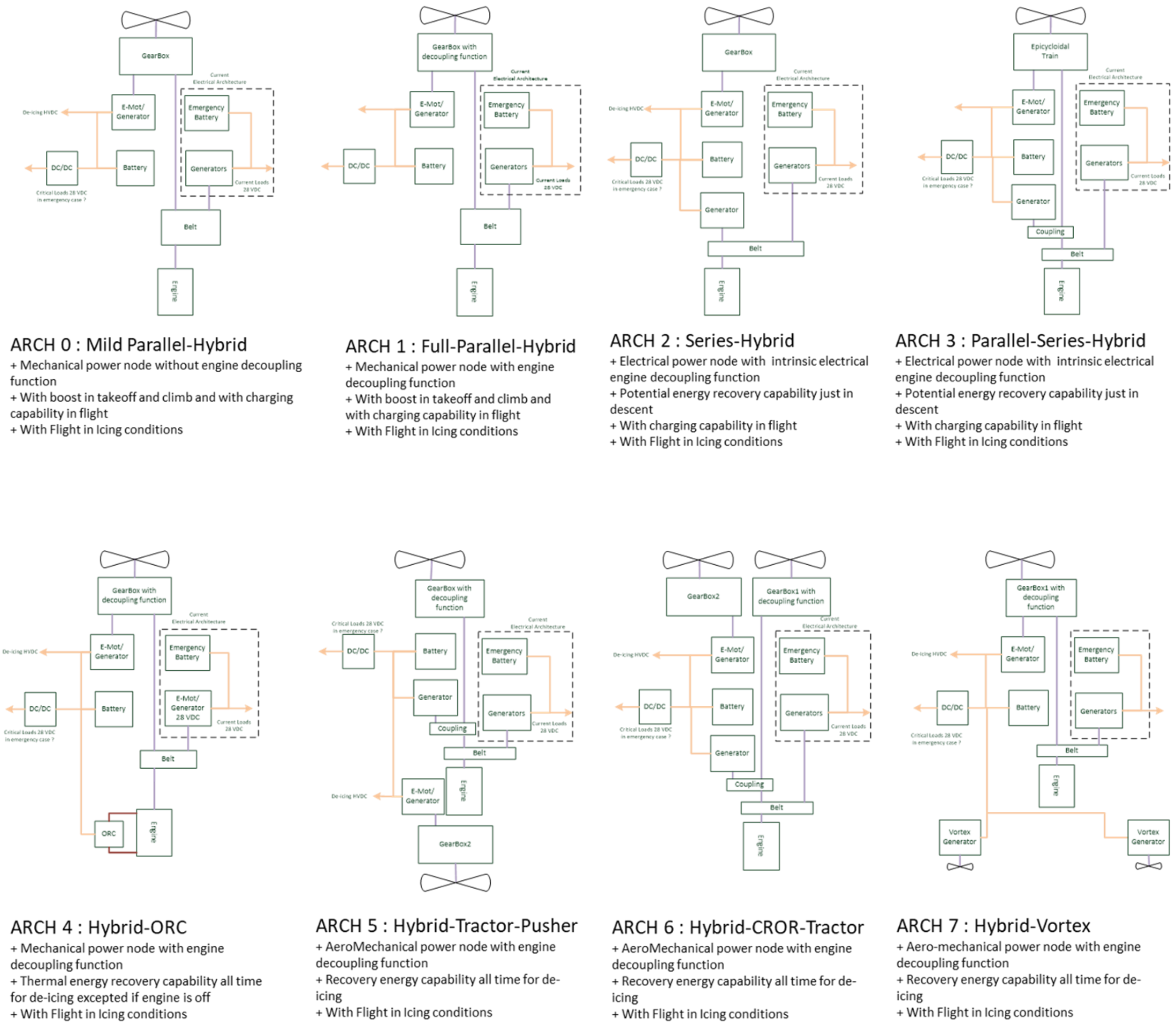

Figure 1-1: Variety of hybrid-electric propulsion and power systems candidates applicable for UAV applications; Carbonneau and Isikveren (2017), originally sourced from Chesneau (2016).

2 SIZING METHODS FOR HYBRID-ELECTRIC PROPULSION AND POWER ARCHITECTURES

As was discussed in the introductory remarks, there are many options to choose when it concerns implementation of hybrid-electric PPS architectural layouts. In order to economise the sheer volume of information necessary to describe methods and models specific to each of the architectures given in Figure 1-1, the authors shall focus on methodologies specific to ARCH 4, i.e. Autarkic-Parallel-HEPPS with the thermal engine integrated with an Organic Rankine Cycle (ORC) machine. Motivation for this choice is expounded in a case study review presented later in this technical paper. Other methods for modelling and constrained optimisation are also reviewed in this section since these aspects are universally applicable, irrespective of the type of hybrid-electric architecture selected. The review of methodology reflects work published by the first author of this technical paper. For further details, the reader is referred to the Masters thesis of Yezeguelian (2019).

2.1 Preamble

The main objective of this study is to find to what extent any HEPPS can increase the maximum endurance of an aircraft, whose fundamental propulsion system and design are retained. It is assumed that the Maximum Take-Off Weight (MTOW, W_{MTOW}) can be increased by some quantity ΔW, which would include structural strengthening for higher loads, incremental mass mostly coming from the PPS increase in bill-of-material, and where applicable, additional fuel. Generally for UAVs, this increment of ΔW is usually limited to a maximum of $+10\% W_{MTOW}$ because any further increases would tend to alter the integrated design in a significant fashion, thus necessitating changes to planform area and/or compelling a selection of a different engine due to power rating considerations.

The sizing methods discussed here are based upon a couple of critical assumptions, in keeping with contemporary UAV qualification practises:

- The Take-Off Distance (TOD) should not be increased when operating at $W_{MTOW} + \Delta W$; and,
- The Time-To-Climb (TTC) should not be increased when taking-off at $W_{MTOW} + \Delta W$.

In an effort to maximise the likelihood of achieving the above mentioned two goals, pertinent control parameters were identified as:

- Boosting mechanical power during Take-off (TO) and Climb (CLB) phases; and,
- Cut-off altitude upon which boosting mechanical power is terminated during the en route climb phase.

Considering the relatively low gravimetric specific energy attributes at system-level of contemporary batteries compared to aeronautical hydrocarbon based fuels (around 0.110 kWh/kg versus 11.9 kWh/kg), at first glance, it appears counter-intuitive to contemplate series or parallel configured HEPPS layouts with purpose to maximise the endurance of an aircraft.

Aligned with the case study shown later in this technical paper that presents practical application of the methods given here, for illustrative purposes, the methodology and models discussed below focus upon implementation of a Parallel-HEPPS architecture, with the thermal engine complemented by an ORC machine.

2.2 Empty Weight Revision

Items specific to any HEPPS channel, such as power electronics, Power Management And Distribution (PMAD), and machines need to be book-kept. For instance, assuming the electric motor runs on Alternating Current (AC), an inverter is necessary to convert the Direct Current (DC) voltage from a battery to an AC voltage supplying the electric motor. Reflecting state-of-the-art, the gravimetric specific power was taken to be 3.0 kW/kg, with a peak efficiency of 95%. In addition, the use of electrically powered equipment within the architecture infers peripheral equipment to address thermal regulation and control requirements. As an example, the prediction of a cooling system mass ($m_{cooling}$) for any electric motor(s) is considered to be a monotonic function of the motor mechanical power, viz.

$$m_{cooling} = d_{cooling}\, P_{thermal} = d_{cooling} \left(\frac{1-\eta_{EM}}{\eta_{EM}}\right) P_{EM} \quad (1)$$

where $d_{cooling}$ is the inverse of gravimetric specific power of the cooling system (kg/W), $P_{thermal}$ is the thermal power to evacuate heat (W), η_{EM} is the mechanical efficiency of the electric motor, and P_{EM} is the mechanical power of the electric motor (W).

Furthermore, due to the additional bill-of-material that constitutes advanced PPS approaches, a revision is necessary to the aircraft empty weight that is beyond simply incremental mass of the components that constitutes the architecture. Any extra ΔW implies account of changes in the loads to all aircraft main structures. Based upon methodology published by Isikveren (2019) and Isikveren and Schmidt (2014) and utilising a database of Tactical UAVs issued by Verstraete and Palmer (2018), a linear model of 0.3 kg/kg_{MTOW} was derived.

2.3 Modelling an Organic Rankine Cycle Machine

The Organic Rankine Cycle (ORC) is described by a rather simple thermodynamic cycle. Based upon recent work done by Zarati, Maalouf and Isikveren (2017) the merits of integrating such machines with existing thermal engines in order to boost performance and improve efficiency were established, and, recommendations were made to investigate feasibility of adopting such an approach in the context of HEPPS.

2.3.1 Description of the ORC Machine

An ORC machine comprises at least a pump, a boiler, a turbine, and a condenser. The aim of this cycle is to convert thermal energy into mechanical energy. In the case of any vehicle generating an exhaust efflux, e.g. an UAV with thermal engine as the power plant, a significant portion of fuel chemical energy is lost in terms of exhaust gases, which are expelled at very high temperatures into the atmosphere. For conventional piston engines, their temperatures can reach up to 1000°C. In order to reuse part of this lost energy, these exhaust gases can be cooled down through the boiler of an ORC in order to loop the generated turbine mechanical power back into the engine shaft. In this case, the pump is driven by the engine shaft, with a Continuously Variable Transmission in order to properly choose a pump rotary speed depending upon the flight phase an aircraft encounters. A schematic and description of the machine attributes together with the details about the process is provided in Figure 2-1.

In accordance with optimisation work based upon dynamic simulation conducted by Yezeguelian (2019) the extent of additional mechanical power for application to light fixed-wing aircraft (similar to Tactical MALE UAVs) employing Parallel-HEPPS was found to be +17% of the original thermal engine. For purposes of the studies presented here this value was declared as an upper bound. In addition, a practical working fluid was proposed by Yezeguelian (2019) to be water, and in the context of UAV application the evaporation and condensation operating temperatures were calculated to be 324°C and 100°C respectively. Basically, for quasi-static analyses purposes, a simplification that can be motivated is to consider the impact of an ORC machine on aircraft performance via a linear gravimetric specific power model, and expected mean shaft power generation credited during CLB and cruise (CRZ) phases only;- during TO it is assumed the cycle would never reach peak operating conditions until the next phase of aircraft operation.

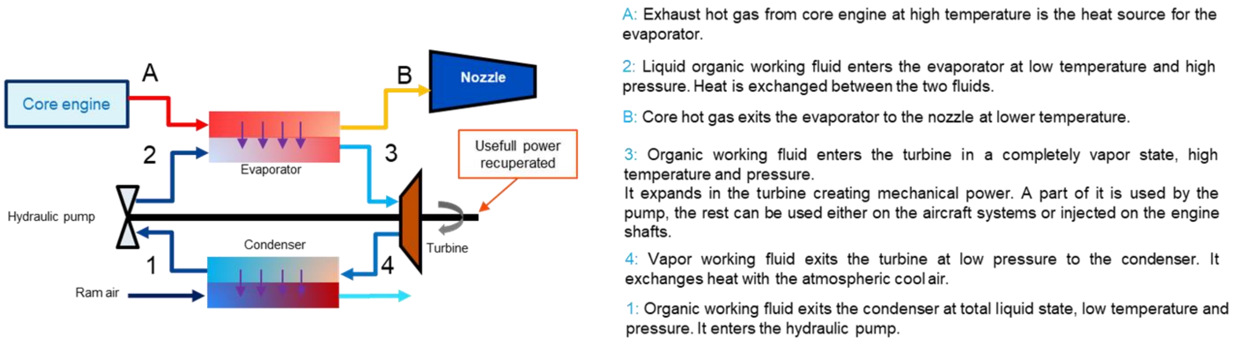

Figure 2-1: Details about an Organic Rankine Cycle machine (Zarati, Maalouf and Isikveren, 2017).

In order to model the mass impact integrating such machines with an existing thermal engine would have, a rudimentary linear model based upon gravimetric specific power characteristics was deemed sufficient. By examining a large regional turboprop, Zarati, Maalouf and Isikveren (2017) studied the mass impact of an integrated ORC machine generating a maximum of around 105 kW (141 hp) for a reference engine producing 1.9 MW (2560 hp) of shaft power. A mass breakdown of the entire installed ORC machine is given in Figure 2-2. Assuming a turbine gravimetric specific power of 0.5 kW/kg, Zarati, Maalouf and Isikveren (2017) established an installed ORC machine gravimetric specific power of approximately 0.35 kW/kg. The critical assumption made for application to UAV aircraft engines is a linear scaling approach for mass estimation would be valid, i.e. 105 kW (141 hp) down to 5 kW (7 hp).

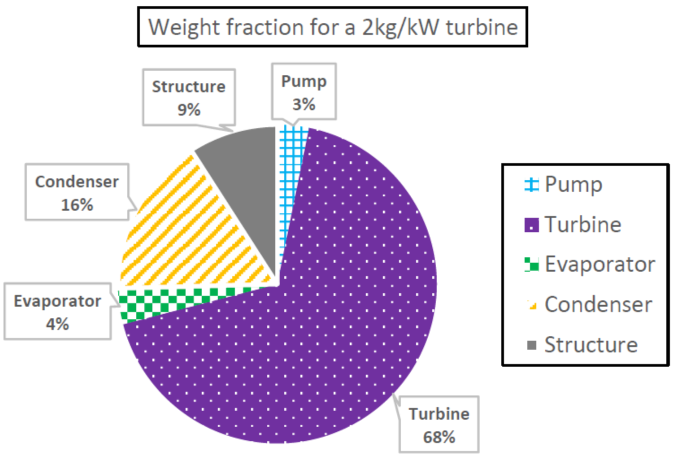

Figure 2-2: Organic Rankine Cycle machine mass breakdown, maximum generated power of 105 kW (Zarati, Maalouf and Isikveren, 2017).

2.3.2 Establishing Power Trades Between an Organic Rankine Cycle Machine and the Parallel-Hybrid-Electric Channel

It would of interest gauge at what level of battery gravimetric specific energy it becomes more advantageous during the CLB phase to hybridise the PPS in favour of the Parallel-HEPPS channel over that of the ORC machine. An alternative characterisation of the problem is to identify the battery system-level gravimetric specific energy that produces a lighter HEPPS channel+ORC combination designed for CRZ compared to ORC-only designed for CLB and CRZ. This threshold of battery system-level gravimetric specific energy can be established algebraically, as exemplified by the following equation

$$e \geq \frac{t_{boost}}{\eta_{EM}\,\eta_{INV}\left[\frac{1}{d_{ORC}} - \frac{1}{d_{EM}} - \frac{(1-\eta_{EM})d_{cooling}}{\eta_{EM}} - \frac{1}{(\eta_{EM}\,\eta_{INV}\,d_{INV})}\right]} \qquad (2)$$

where e is the battery system-level gravimetric specific energy (Wh/kg), t_{boost} is the duration of boost at CLB (h), d_{ORC} is the gravimetric specific power of an ORC machine (W/kg), d_{EM} is the gravimetric specific power of the electrical machine (W/kg), η_{EM} is the electrical machine efficiency, η_{INV} is the inverter efficiency, and d_{INV} is the inverter gravimetric specific power (W/kg).

2.4 Modelling an Installed De-icing System

Generally, icing conditions are said to exist if the Total Air Temperature is less than 10°C from sea level up to an altitude of 22000 ft. Figure 2-3 provides information about typical operating conditions in which Tactical MALE UAVs are expected to operate.

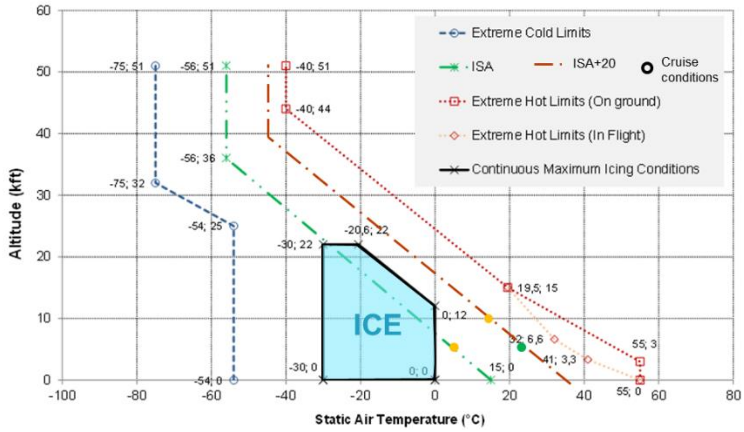

Figure 2-3: Extremities in operating conditions for typical Tactical MALE UAVs.

When considering Tactical MALE UAVs, de-icing of the wing and empennage surfaces cannot be accomplished by means of bleed air based piccolos due to limitations imposed by the propulsion system. Instead, only electrical heaters are considered to be appropriate (Figure 2-4 as an example). A simple model of the maximum power required to sustain de-icing capability is offered by Meier and Scholz (2010). The extent of thermal power that needs to be imparted upon a surface for purposes of de-icing was taken as 6.0 kW/m^2. Electrical-to-thermal power conversion was assumed to be 80%, as per the recommendation of Meier and Scholz (2010).

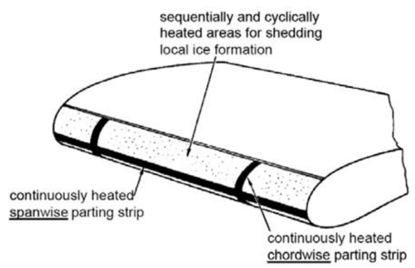

Figure 2-4: Arrangement for de-icing mats (Meier and Scholz, 2010).

2.5 Take-off and Climb Power Schedule Optimisation: Adapted Raymer's Method

Albeit modified, methods developed by Raymer (2012) were used as a foundation to handle analysis compatible with Parallel-HEPPS architectural attributes. Fundamentally, Raymer's method works off the premise energy expenditure is completely transformed into mass reduction of the aircraft with time, whereas the HEPPS channel is characterised as fixed mass irrespective of energy expenditure. A further complication to this scheme occurs because not only should appropriate levels of shaft power boost during TO and CLB phases be identified, but the cut-off altitude upon which boosting is terminated during the CLB phase is required as well.

The iterative scheme, which loops after an initial guess of Take-Off Weight (TOW) is illustrated in the following block diagram:

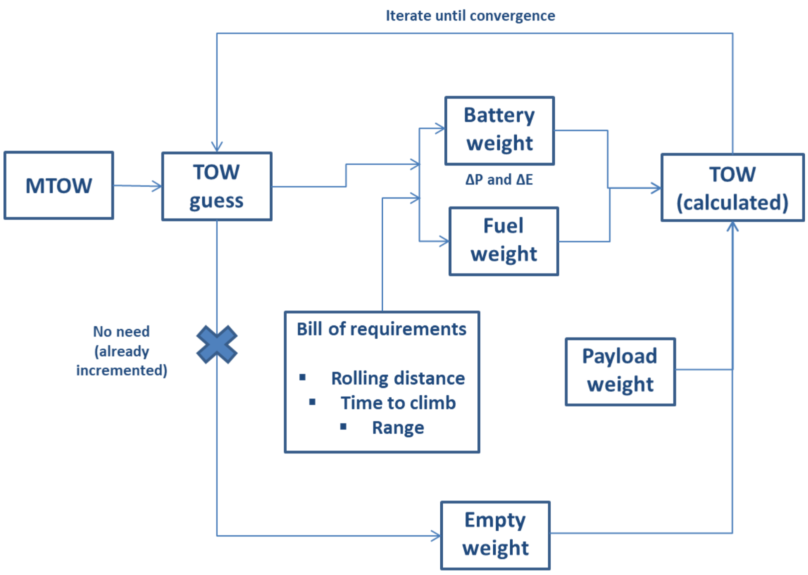

Figure 2-5: Adapted Raymer's method routine.

When developing such a customised methodology it is necessary to assess both the additional power and energy that should be provided by the additional propulsive system in order to fulfil the given constraints of TOD and TTC not being exceeded compared to a baseline aircraft. Using the two equations related to TO and CLB given below, requisite battery and electric motor and PMAD masses can be computed assuming a variety of gravimetric specific power and gravimetric specific energy values. Focusing on TO, the TOD can be predicted using

$$S_{run} = \frac{1}{2g}\int_0^{V_{LOF}^2} \frac{dV^2}{\frac{TV}{W_O} - \mu - (C_D - \mu C_L)\frac{\rho V^2 S}{2W_O}} \quad (3a)$$

And upon integration, this expression reads as

$$S_{run} = \frac{V_{LOF}^2}{2g\left(\frac{TV_{LOF}}{W_O} - \mu'\right)} \quad (3b)$$

where S_{run} is the rolling distance (m), g is the gravitational acceleration (m/s²), $V_{LOF} = 1.1\ V_{S1g}$ is the characteristic speed at take-off (m/s), V_{S1g} is the 1g stall speed of the aircraft at ground level (m/s), T is the thrust generated by the aircraft engines at take-off (N), W_o is the aircraft take-off weight (N), μ is the friction coefficient of the runway, C_D is the drag coefficient, C_L is the lift coefficient, ρ is the air density (kg/m^3), S is the wing reference area (m²), and μ' is given by Torenbeek (1982) as μ' = 0.02 + 0.01C_{LTO} with C_{LTO} being the operating lift coefficient of the aircraft at V_{LOF}. The required shaft power, P_r (W), is calculated with

$$P_r = V_V W + \frac{1}{2}\left(\rho V^3 S C_{Do} + \frac{4KW^2}{\rho V S}\right) \quad (4)$$

where V_V is the target rate of climb (m/s), W is the aircraft weight (N), C_{Do} is the zero-lift drag coefficient, and K is the vortex-induced drag factor.

2.6 PaceLab Aircraft Preliminary Design (APD)

The second step of the quasi-static analysis is to assess the performance of the hybrid aircraft using preliminary design software, namely PaceLab Aircraft Preliminary Design, or APD (APD TXT e-solutions, 2019). Through geometry, mass definitions, propulsion and mission characteristics as inputs PaceLab APD makes it possible to retrieve performance characteristics from time history table reports and graphs.

The main problem with this software is it does not facilitate features that handle HEPPS architectural configurations. It is mainly based upon a complex combination of Torenbeek (1982) and Raymer (2012) methods, which do not make it possible to model hybrid propulsion due to absence of judiciously declaring fixed mass in relation to the HEPPS channel performance with respect to time. Therefore, it was decided to modify the software method in order to include components to take electrified propulsion into consideration.

Thrust tables were developed for the electric motor in order to comply with the software format. The batteries, which should be recharged as fast as possible during CRZ (in order to use the electric motor as a back-up system in case of engine failure), were modelled as a mass in aircraft equipment, and the impact of recharge on aircraft performance was assessed with an incremental fuel supply segment: a certain amount of fuel is directly used for recharge, at a certain rate, depending upon the amount of energy and power to recharge. Analytically, this aspect is modelled using equations

$$m_{fuel} = \frac{E_{bat}}{e_{fuel}\,\eta_{ICE}\,\eta_{EM}} \quad (5)$$

$$\frac{dm_{fuel}}{dt} = \frac{P_{EM}}{e_{fuel}\,\eta_{ICE}} \quad (6)$$

where m_{fuel} is the fuel mass to be provided for battery recharge (kg), E_{bat} is the battery energy to recharge (J), e_{fuel} is the fuel specific energy (kg/J), and η_{ICE} is the combustion engine mechanical efficiency.

Figure 2-6 provides a screenshot of the mission profile defined using PaceLab APD. The software methods were modified to include a Boolean parameter for the climb block, in order to allow, or discard, an electrical sourced shaft power boost feature. With the PaceLab APD software, it is also possible to run a variety of trade-studies. In order to find an optimal power and cut-off altitude combination, a trade-study was executed with the following characteristics:

- Sizing parameters: boost cut-off altitude, which corresponds to the altitude at which the first boosted CLB segment ends and the second non-boosted commences
- Optimisation variable: endurance (or loiter segment time)
- Constraints: TOD and TTC

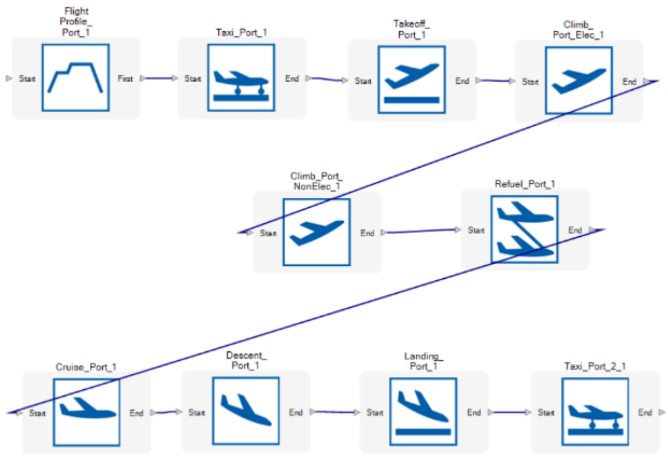

Figure 2-6: PaceLab APD hybrid-electric power and propulsion system aircraft mission profile.

2.7 Constrained Optimisation Algorithm

It was decided to manually implement a method in order to check the PaceLab APD results. The algorithm was implemented in Python (Python Software Foundation, 2019), and consists in a time-dependent model, adapted from Riboldi (2018). The differential equations were solved solely in their integral form, so the value of each variable was computed at each numerical time step. For instance,

$$W_{fuel} = W_{fuel,0} - \int_0^t \frac{\sigma_{ICE}\, P_{ICE}\, g}{e_{fuel}\, \eta_{ICE}} d\tau \qquad (7)$$

where W_{fuel} is the fuel weight (N), $W_{fuel,0}$ is the initial fuel weight (N), σ_{fuel} is the combustion engine throttle setting, and P_{ICE} is the combustion engine shaft power (W).

The cost function to minimise was declared as the following:

$$\left(\frac{W_{EM}}{W_{EM-ref}}\right)^2 + \left(\frac{W_{bat}}{W_{bat-ref}}\right)^2 \qquad (8)$$

where W_{EM} is the electric motor weight (N), W_{bat} is the battery pack weight (N), and the reference values are extracted from PaceLab APD trade study results. This cost function minimisation is equivalent to minimising the added system weights. Extending beyond PaceLab APD capabilities, this algorithm can directly consider battery State Of Charge (SOC), hence any requirements to conduct recharging operations.

3 CASE STUDY: EULAIR TACTICAL MALE DRONE VARIANT

In order to elucidate the discussed methodology and how it can be applied in practical terms, an example hybrid-electric propulsion system sizing was performed on the proposed Eulair Tactical MALE Drone, which is taken to be a major variant of the original Eulair Twin2 light-sport aircraft platform.

3.1 Description of the Twin2 Aircraft Platform

Designed in France the Twin2 platform is a two-passenger, side-by-side, light-sport aircraft configured as a two-engine tractor-pusher and incorporates a tandem wing arrangement. The Twin2 has a forward-mounted low-set control canard and an aft-mounted high-set main wing. Yaw control is facilitated by so-called crocodile rudders integrated with the winglets of the main wing. Figure 3-1 displays a general arrangement in conjunction with a rendered isometric view and photograph of the aircraft in operation (Eulair, 2019a).

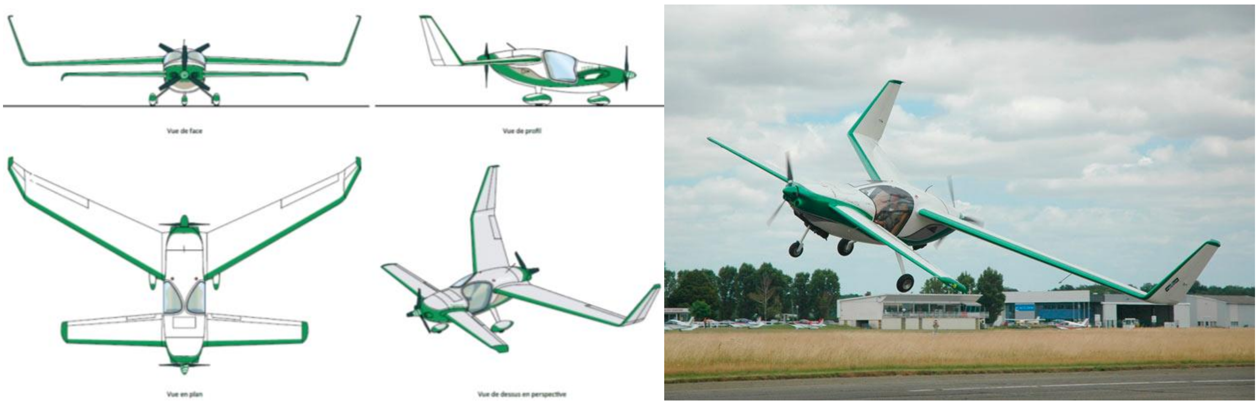

Figure 3-1: The Eulair Twin2 light-sport aircraft platform; Eulair (2019a).

This minimum structural mass solution maximises synergy in terms of overall aerodynamic performance, and, handling and control. The twin engine approach is purported to dramatically minimise the probability of a complete propulsion system catastrophic failure. In addition, due to the tractor-pusher arrangement placed upon the aircraft centre-line whenever a One-Engine Inoperative condition occurs aircraft asymmetry is kept to a minimum. The twin-engine approach also has the benefit of avoiding propeller strike of the aft mounted pusher propulsion system due to a shorter propeller diameter.

Eulair currently offers two different engine options for the Twin2 platform, namely, with two Rotax 503 2Cs, or, two Hirth F23 LW (two-stroke piston engine). A hybrid-electric version is planned, with one thermal engine mounted in the forward fuselage and an all-electrically driven propeller mounted at the aft-fuselage. Futhermore, a tactical MALE drone with one diesel engine as a pusher is stated.

3.2 Description of the Tactical MALE Drone Variant

When examining current offerings of Tactical MALE drones, according to NATO (2009) typical maximum endurance is 24-48 hours, such aircraft weigh 1000-1500 kg (2200-3300 lbm), and loiter/cruise in the vicinity of 3000 m (10000 ft). Figure 3-2 presents general characteristics of UAVs according to twelve categories as proposed by van Blyenburgh (2006) in terms of range and endurance. The purpose of this particular exercise was to find an architectural solution that significantly enhances the integrated performance attributes (increase endurance and maximum range) of Tactical MALE drones without altering the Outer Mould Lines (OMLs), or external lines, of the baseline aircraft.

The first step was to generate a Tactical MALE drone version of the Twin2 light-sport aircraft, hereafter labelled as the “Baseline Drone”. Although the amount of information regarding a drone variant was somewhat lacking, the authors decided to produce a major variant by initially modelling the original Twin2 according to an appropriate level of conformity to information disseminated by Eulair (Eulair, 2019b and 2019c). From this model of the Twin2 platform, based upon previously published information by Eulair and media articles (Eulair, 2019a, and Aerobuzz, 2017) in conjunction with a series of posits made by the authors aircraft specifications for the Tactical MALE baseline were produced. A comparison and contrast between the platform Twin2 and Baseline Drone aircraft is offered in Table 3-1.

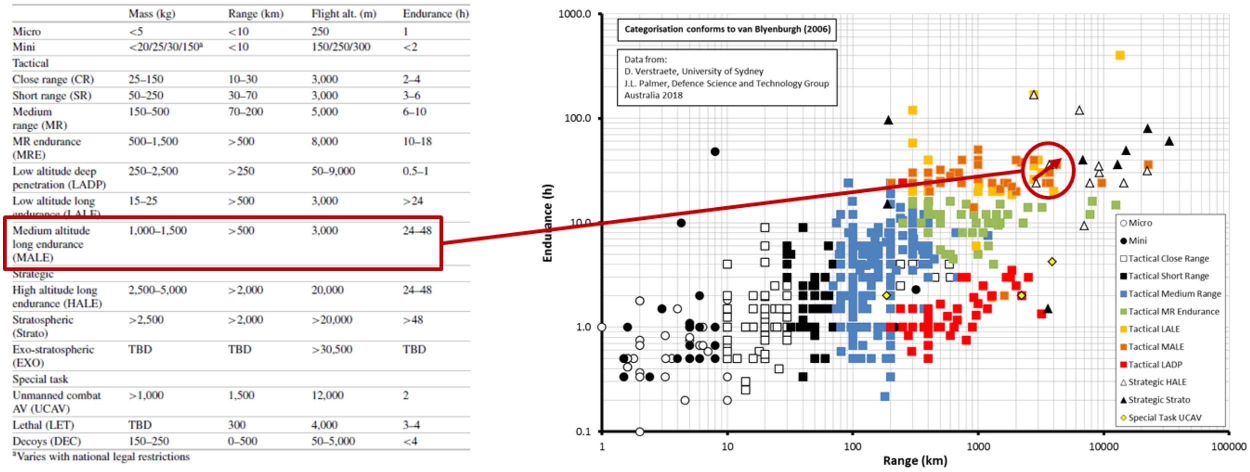

	Mass (kg)	Range (km)	Flight alt. (m)	Endurance (h)
Micro	<5	<10	250	1
Mini	<20/25/30/150[a]	<10	150/250/300	<2
Tactical				
Close range (CR)	25–150	10–30	3,000	2–4
Short range (SR)	50–250	30–70	3,000	3–6
Medium range (MR)	150–500	70–200	5,000	6–10
MR endurance (MRE)	500–1,500	>500	8,000	10–18
Low altitude deep penetration (LADP)	250–2,500	>250	50–9,000	0.5–1
Low altitude long endurance (LALE)	15–25	>500	3,000	>24
Medium altitude long endurance (MALE)	1,000–1,500	>500	3,000	24–48
Strategic				
High altitude long endurance (HALE)	2,500–5,000	>2,000	20,000	24–48
Stratospheric (Strato)	>2,500	>2,000	>20,000	>48
Exo-stratospheric (EXO)	TBD	TBD	>30,500	TBD
Special task				
Unmanned combat AV (UCAV)	>1,000	1,500	12,000	2
Lethal (LET)	TBD	300	4,000	3–4
Decoys (DEC)	150–250	0–500	50–5,000	<4

[a]Varies with national legal restrictions

Figure 3-2: Survey of a variety of UAVs, associated performance, and general specifics in relation to tactical MALE drones (Isikveren, 2018); table on left is from NATO (2009); chart data on right is from Verstraete and Palmer (2018).

Table 3-1: General aircraft specifications of the Eulair Twin2 and Baseline Drone.

Characteristic	Light-Sport Twin2	Baseline Drone
MTOW (kg / lbm)	472* / 1041	900* / 1984
Empty Weight (kg / lbm)	270* / 595	450* / 992
Engine Max. Power, ISA, s.l. (kW / hp)	2 x 37* / 50	104 / 139
Propeller(s) Diamater (m / in.)	1.52 / 60	1.67 / 66
Stall Speed, 1g, ISA, s.l. (kph / KTAS)	65* / 35	90 / 49
Take-off distance (m / ft)	150* / 492	291 / 954
Max. Rate of Climb, All-Engines, ISA, s.l. (ms^{-1} / fpm)	5.0* / 984	5.0* / 984
Cruise Altitude (m / ft)	2000* / 6560	5000* / 16400
Time-to-Climb (mins)	5	19
Payload for Mission (kg / lb)	162* / 357	132 / 292
Max. Endurance Speed, ISA (kph / KTAS)	111 / 60	171 / 92
Maximum Endurance, loiter segment, ISA (h)	3.3	25.0*
Max. Range Speed, ISA (kph / KTAS)	163 / 88	215 / 116
Maximum Range, ISA (km / nm)	478 / 258	5118 / 2764
Typical Cruise Speed, ISA (kph / KTAS)	200* / 108	185 / 100
Range, Typical Cruise, ISA (km / nm)	450* / 243	4731 / 2554
Max. Cruise Speed, ISA (kph / KTAS)	240* / 130	220 / 119

* denotes values given by Eulair in publically disseminated documentation

It should be noted that for the Baseline Drone the original Eulair specification stated incorporation of a single 90 hp (67 kW) diesel engine compatible for aeronautical applications. During the major variant transformation from the Eulair Twin2 platform to the Baseline Drone, investigations showed a single 104 kW (139 hp) engine would be required in order to meet the critical performance specifications of maximum rate-of-climb of 5.0 m/s (984 fpm) and 25 hours maximum endurance during the loiter segment at 5000 m (16400 ft) altitude.

3.3 Description of the Baseline Drone with Advanced Propulsion and Power Systems

Prior to commencing with propulsion system sizing and constrained optimisation activities, a set of objectives and requirements were fashioned. The main objectives are outlined as follows:

- Maximise endurance by +20% compared to the Baseline Drone
- Implementation of a de-icing device such that useful missions can be undertaken even when en route icing conditions are encountered
- Ability of the aircraft to land intact after engine inoperative – called “Aircraft Recovery”
- If the advanced propulsion system solution employs hybrid-electric propulsion, it is required to be autarkic in nature, i.e. ready to dispatch all missions without the need for external recharge or replacement of battery

A number of requirements and build strategy constraints were also declared:

- The target vehicle is to be a variant of the Baseline Drone, of which is a major variant of the original Eulair Twin2 light-sport aircraft. A variant is taken to be development of a new aircraft product via the increase (or decrease) of take-off gross weight, incorporation of enhancements through any equipment/amenities upgrade, and most importantly, does not generate any significant change to the baseline aircraft OMLs
- An equality constraint of the final design MTOW equal to 110% of the Baseline Drone is to be imposed
- Capacity of the Baseline Drone existing fuel tanks are open to revision, namely, scope for maximum capacity increase in the final design is permissible
- The original Baseline Drone thermal engine is to be retained, i.e. maximum rating of 104 kW (139 hp) not to be altered
- The Baseline Drone Take-Off Distance (TOD) and Time-To-Climb (TTC) are not to be exceeded
- All equipment and technological development needs to be compatible with a Technology Readiness Level (TRL) of 6 by no later than year-2023

The scheme presented in this technical paper involves a simple build strategy that involves fixing the airframe OMLs of the Twin2 in order to produce a Tactical MALE drone major variant but with a single engine and propeller. Upon careful review of the eight architectural candidates given in Figure 1-1, ARCH 4, namely, one in which the thermal engine is integrated with an ORC machine and subsequently configured in a parallel-hybrid arrangement, was adopted for investigative work. The Variant Autarkic-PARallel-hybrid-electric Eulair drone, or VAPARE, has the additional benefit of facilitating a de-icing system function and assisting the aircraft during engine-inoperative mode with electrically driven propeller capability, albeit with curtailed extent of time aloft. The build strategy is illustrated in Figure 3-3.

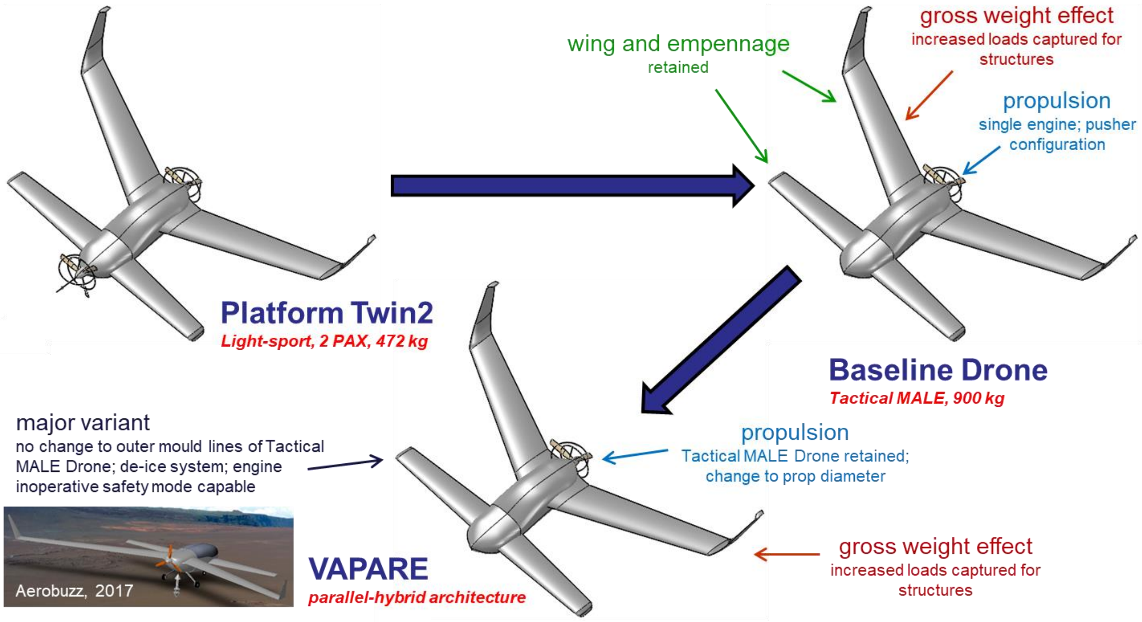

Figure 3-3: Build strategy of Baseline Tactical MALE Drone and subsequent hybrid-electric propulsion and power system variant.

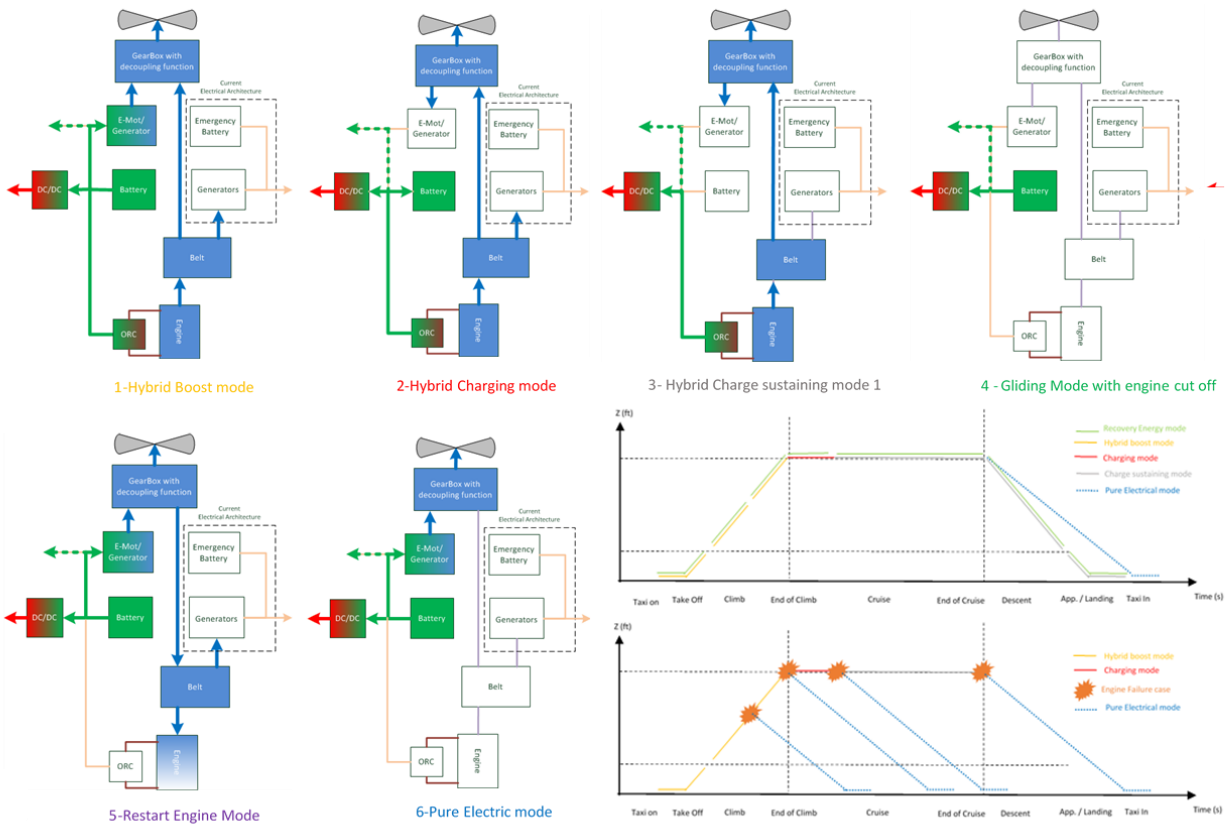

Figure 3-4: Various normal and abnormal operating modes of the VAPARE architecture; Carbonneau and Isikveren (2017), originally sourced from Chesneau (2016).

Correspondingly, whenever hybrid-electric architectures are considered for advanced PPS it is of utmost importance to describe the activity state of said architecture according to a set of operational modes the aircraft is expected to encounter. Appropriate definitions for the operating modes of the aircraft relies upon a thorough understanding of not only the mission flight profile but establishing when certain functions of the hybrid-electric architecture, whether related to propulsion or non-propulsive systems, will activate/shut-down during both normal and abnormal modes of operation. For the selected VAPARE architecture, six operating modes were identified and then related to the mission profile. These are illustrated in Figure 3-4.

From an adaptation of the dynamic analysis published by Yezeguelian (2019) for the ORC machine, the expected mean generated mechanical power at CLB was calculated to be 18 kW (24 hp), and correspondingly, 5.0 kW (6.7 hp) during the loiter segment. This represents a contribution of +17% during CLB and +16% during loiter. The 18.0 kW during CLB constitutes a maximum value of shaft power injection in order to meet the TTC constraint – this means any combination of values contributed by battery and/or ORC machine must tally at least 18 kW.

An initial estimate of 8.8 kW (11.7 hp) with regards to the de-icing system maximum power requirement was predicted to be a total mass of 10 kg (22 lbm), which includes the equipment and wiring.

3.4 Results of the Quasi-static Analysis and Optimisation Studies

In order to fully appreciate and understand the pathway in realising an overall performance improvement outcome for VAPARE(IV), which represents the Baseline Drone integrated with ORC and configured as an Autarkic-Parallel-HEPPS thus facilitating TO/CLB boost, in-flight recharge, de-icing, and aircraft recovery capability, a series of integration scenarios were examined, each building upon the last. To this end, integration scenario results to be presented in this section are given as

Table 3-2: Integration scenarios considered for VAPARE investigation.

Scenario	PPS Enhancement versus Baseline Drone	Boost TO and CLB	In-flight Recharge	De-ice System	Aircraft Recovery System
VAPARE(I)	Parallel-Hybrid-Electric	Yes	Yes	No	Yes
VAPARE(II)	ORC	No	No	Yes	No
VAPARE(III)	Parallel-Hybrid-Electric + ORC	Yes	Yes	No	Yes
VAPARE(IV)	Parallel-Hybrid-Electric + ORC	Yes	Yes	Yes	Yes

3.4.1 Constrained Power Schedule Optimisation of Parallel-Hybrid-Electric Channel

For VAPARE(I), (III) and (IV) scenarios an optimal power schedule (degree-of-hybridisation and cut-off altitude) specific to the Parallel-HEPPS channel was identified. It is highlighted constraints of TOD and TTC were applied to the mathematical search activity. As previously discussed the analytical basis in achieving the desired outcome was accomplished using the modified Raymer's Method, serving as a primer for establishing appropriate degree-of-hybridisation and cut-off altitude, thereafter executing the prescribed power schedule using PaceLab APD in order to quantify the integrated operational performance result. An interesting observation was both the level of degree-of-hybridisation together with the cut-off altitude were very similar for VAPARE(I), (III) and (IV) scenarios. A sample, which provides a notional understanding of the results is shown in Table 3-3 indicating an expected degree-of-hybridisation and cut-off altitude of 12-14% and 10500-

12500 ft respectively. It should be noted the optimisation scheme was subject to the following bounded constraints and convergence criteria:

- The battery SOC was bounded between 20% and 90% in order to ensure optimal performance and secure practical limit in terms of battery life (1500-2000 cycles); and,
- A tolerance of 1.0 min for TTC, and, 2.0 m for the TOD in order to secure convergence.

Table 3-3: Sample of PaceLab APD control parameters sensitivity study results.

	Design Parameters		Objective variable			Constraints	
Point n°	Hybrid. factor	Cut-off alt (ft)	Endurance (h)	MTOW variation	Recharge time (min)	TTC (min)	Rolling distance (m)
138	12%	11483	24.7	+10%	27	19.2	285.4
232	15%	9843	24.6	+10%	21	18.8	296.5
76	11%	13123	24.6	+10%	33	21.2	277.3
107	12%	12303	24.6	+10%	30	19.7	281.4
185	14%	10663	24.6	+10%	23	19.0	291.0
437	20%	7382	24.6	+10%	13	17.8	318.0
358	18%	8202	24.6	+10%	15	18.1	310.1
532	22%	6562	24.6	+10%	11	19.4	327.0
295	17%	9022	24.5	+10%	18	18.4	303.5
30	9%	14764	24.5	+10%	41	20.7	271.1
548	23%	6562	24.4	+10%	11	17.3	328.3

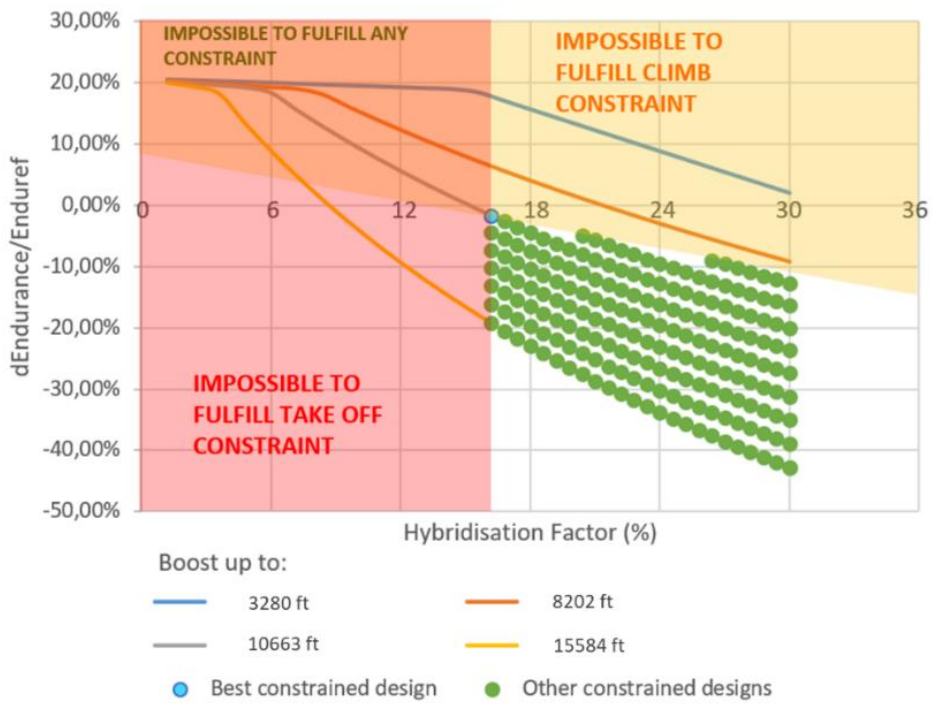

Figure 3-5: PaceLab APD post-processed graphical result.

An example of optimisation post-processing for VAPARE(I), i.e. an Autarkic-Parallel-HEPPS only architecture, is presented in Figure 3-5. The point of such a graphical representation is to allow the designer/analyst to understand the influence TOD and TTC have with regards to a given integrated maximum endurance outcome. Iso-lines of cut-off altitude are indicated together with zones of infeasibility. It can be seen degree-of-hybridisation values less that 16% means the TOD constraint is always violated, and with increasing degree-of-hybridisation beyond 16% cut-off altitudes below 8200-10700 ft do not fulfil the TTC requirement. The blue dot in Figure 3-5 shows the best constrained outcome. As a general observation, any Autarkic-Parallel-HEPPS architectures utilised for VAPARE are likely to not generate an increase in maximum endurance compared to the Baseline Drone. The reason for this attributable to relatively small fraction of fuel expended for CLB: any reduction in fuel during this phase of flight is easily overwhelmed by the higher all-up-weight (thus, drag) of the aircraft during the loiter segment.

3.4.2 VAPARE Drone Results and Discussion

Results of all scenarios shown in Table 3-2 together with data indicative of the Baseline Drone and the original platform Eulair Twin2 are presented in Table 3-4.

Table 3-4: Results generated for a variety of VAPARE integration scenarios contrasted against the Baseline Drone and the original Eulair Twin2 platform.

	Twin2	Drone	VAPARE(I)	VAPARE(II)	VAPRE(III)	VAPARE(IV)
Take-off Engine Power, kW	75	104	104	104	104	104
Maximum ORC Power, kW	n/a	n/a	n/a	18	5	5
Maximum Battery (at Motor), kW	n/a	n/a	20	n/a	13	13
CLB Power Cut-off Altitude, ft	n/a		10700	n/a	10700	
Propeller Diameter, m	1.52	1.67	1.70			
Wing Loading, kg/m^2	31.5	60.0	66.0			
Reference Wing Area, m^2	15.0					
MTOW, kg	472	900	990			
Delta MTOW	-48%	0	+10%			
Empty Weight, kg	270	450	556	548	523	533
Delta Empty Weight	-40%	0	+24%	+22%	+16%	+18%
Maximum Payload, kg	162	132				
Battery+PMAD+Motor Mass, kg	n/a	n/a	65	n/a	28	28
ORC Mass, kg	n/a	n/a	n/a	51	14	14
Maximum Fuel Mass, kg	40	318	302	310	335	325
Take-off Distance, m	150	291				
V_{S1}, KTAS	35	49	51			
Max ROC, ISA, s.l., fpm	984	984	1136	1101		
Max Operating Altitude, ft	6560	16400				
Time-to-Climb, CRZ Altitude, mins	5	20				
Max. CRZ Spd, KTAS	130	119				
Max Range Spd, KTAS	88	116	117			
Max. Range, nm	258	2764	2467	2938	3181	3071
Delta Max. Range, nm	-91%	0	-11%	+6%	+15%	+11%
Max. Endurance Spd, KTAS	60	92	102	92		
Max. Endurance, loiter seg., h	3.3	25.0	23.5	27.0	30.0	27.8
Delta Endurance	-87%	0	-6%	+8%	+20%	+11%

Inspection of propeller diameters for each of the VAPARE scenarios showed very similar results to one another. For sake of simplification, all scenarios were assigned the same propeller diameter value of 1.70 m (67 in.). A check for propeller strike was conducted in order to ensure rotation/de-rotation during low-speed operations would not be impeded. A clearance of at least 305 mm (12 in.) was set as the minimum allowable; a propeller diameter of 1.70 m produced 457 mm (18 in.), which is in compliance.

Review of empty weights for each of the VAPARE drone candidates shows the Autarkic-Parallel-HEPPS only version is the heaviest with +24% versus the Baseline Drone. The lightest option is the VAPARE(III) with an Autarkic-Parallel-HEPPS+ORC configuration at +16%, and with the option of implementing a de-icing system VAPARE(IV) was estimated to be +18% versus the Baseline Drone.

Observation of optimal speed schedules for maximum range and maximum endurance shows a measure of synchronicity between the Baseline Drone and VAPARE(II)/VAPARE(III)/VAPARE(IV). The outlier is the Autarkic-Parallel-HEPPS only VAPARE(I) when it concerns the maximum endurance speed schedule. The higher wing loading together with no shaft power injection due to absence of an ORC machine during loiter conspire to increase the speed from 92 KTAS to 102 KTAS.

The VAPARE(I) analysis as shown in Table 3-4 assumed a battery gravimetric specific energy of 110 Wh/kg (0.067 hp.h/lbm) at system-level, and the electrical motor was assumed to have a gravimetric specific power of 1.6 kW/kg (0.97 hp/lbm), which are typical in terms of what constitutes state-of-the-art technology. This resulted in a reduction in maximum endurance of 1.5 hours. The main reason for the degradation in performance is a requisite Parallel-HEPPS powertrain mass of 65 kg (143 lbm) to meet TO/CLB specifications, and a for an equality constraint of MTOW = 990 kg (2183 lbm), 16 kg (35 lbm) of fuel compared to the Baseline Drone needed to be removed. Upon completion of a sensitivity study (see Figure 3-6), analysis showed maximum endurance parity with the Baseline Drone could be achieved using a battery with attribute of 160 Wh/kg (0.097 hp.h/lbm) at system-level. If a battery with gravimetric specific energy of 250 Wh/kg (0.152 hp.h/lbm) at system-level could be developed to TRL6 by year-2023, i.e. very optimistic target for Li-S technology, a modest increase of 1 hour to 26 hours maximum endurance is conceivable. The conclusion was a Parallel-HEPPS variant of the Baseline Drone is not considered to be a worthwhile venture.

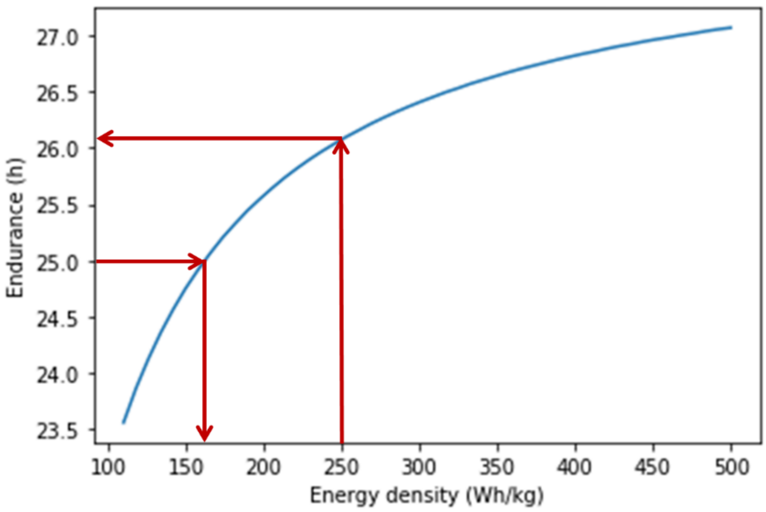

Figure 3-6: Sensitivity of maximum endurance with battery gravimetric specific energy at system-level for VAPARE(I).

VAPARE(II), which does not support aircraft emergency recovery capability but facilitates a de-icing function was found to improve the maximum endurance by almost 2 hours compared to the Baseline Drone. The ORC machine serves a dual purpose of converting mechanical into electrical power using a generator (to operate the de-icing system) as well as injecting shaft power during TO/CLB (18 kW, 24 hp) and CRZ (5.0 kW, 6.7 hp) flight phases.

An extension to VAPARE(II) with an Autarkic-Parallel-HEPPS power-train constitutes VAPARE(III). This particular configuration does not support a de-icing system, but does allow for TO/CLB/CRZ shaft power injection, in-flight recharging and Aircraft Recovery system. Table 3-4 indicates there is potential to meet the

30 hours requirement for maximum endurance provided a battery with gravimetric specific energy of 140 Wh/kg (0.085 hp.h/lbm) is utilised as verified with application of Eqn (2). The result obtained was 138 Wh/kg (0.084 hp.h/lbm), which means for any selected battery system-level gravimetric specific energy exceeding 138 Wh/kg, the ORC machine should cater for CRZ only (provides the 5.0 kW, 6.7 hp), therefore, provides only 5 kW during CLB. For this case, 13.0 kW (17.4 hp) at the motor is needed (supplied by the battery).

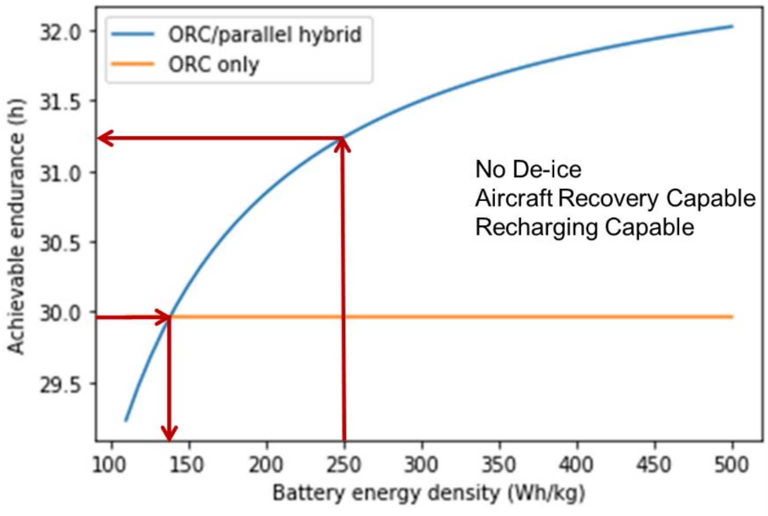

Figure 3-7: Sensitivity of maximum endurance with battery gravimetric specific energy at system-level for VAPARE(III).

An immediate observation is the final design, VAPARE(IV), does not meet the 30 hrs maximum endurance time requirement. In contrast, VAPARE(III), which adopts the same PPS configuration as VAPARE(IV) manages to meet the maximum endurance requirement but does not facilitate a de-icing function. In fact, implementation of a de-icing capability penalises maximum endurance by over 2 hours.

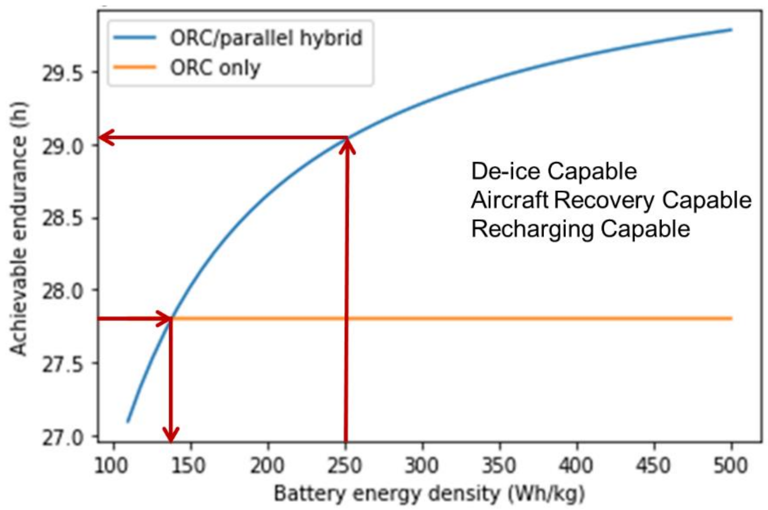

Figure 3-8: Sensitivity of maximum endurance with battery gravimetric specific energy at system-level for VAPARE(IV).

4 CONCLUSION

The aim of this investigation was to produce a variant of a Tactical Medium Altitude Long Endurance Unmanned Aerial Vehicle (UAV), dubbed the Baseline Drone, derived from the original light-sport Eulair Twin2 aircraft. The primary requirement was to realise a 20% increase in the maximum endurance compared to that of the predicted Baseline Drone subject to constraints of retaining the take-off distance and time-to-climb to loiter altitude. Special purpose quasi-static methods were developed in order to optimise power schedules and identify an appropriate cut-off altitude for the selected Autarkic-Parallel-Hybrid-Electric Propulsion and Power System with the thermal engine augmented by an Organic Rankine Cycle (ORC) machine. For this study, with the outer mould lines fixed, the goal was to increase endurance without increasing the Baseline Drone Maximum Take-Off Weight beyond +10%. Studies have shown with state-of-the-art or even projected battery technologies, due to limitations of gravimetric specific energy, it is unlikely the maximum endurance of the Baseline Drone will be increased by adopting an Autarkic-Parallel-HEPPS alone. Results showed that an Autarkic-Parallel-HEPPS architecture coupled with an ORC thermal energy recovery apparatus and high-end year-2020 battery, the endurance of the considered aircraft could be increased by 11%, i.e. a total of 28 hours, including de-icing system, in-flight recharge, and emergency aircraft recovery capabilities. The same aircraft with the de-icing functionality removed resulted in a 20% increase in maximum endurance to 30 hours.

5 BIBLIOGRAPHY

[1] Aerobuzz (2017), “L’ULM bimoteur Twin2 prêt à être commercialisé”, available at: https://www.aerobuzz.fr/breves-aviation-generale/lulm-bimoteur-twin2-pret-a-etre-commercialise/ (accessed 16 July 2019)

[2] Carbonneau, X., Isikveren, A.T. (2017), “ISAE-SUPAERO and SAFRAN HyPAV Perspectives”, Workshop No. 1, 15-16 May 2017, Exploratory Team AVT-ET-173 Hybrid/Electric Propulsion for Airborne Vehicles (HyPAV), Applied Vehicle Technology Panel, Science and Technology Organization, NATO.

[3] Chesneau, G. (2016), SAFRAN Group internal report covering hybrid-electric architectures for Unmanned Aerial Vehicles. Not available for public dissemination.

[4] Committee on Propulsion and Energy Systems to Reduce Commercial Aviation Carbon Emissions (2016), “Commercial Aircraft Propulsion and Energy Systems Research: Reducing Global Carbon Emissions”, Division on Engineering and Physical Sciences, Aeronautics and Space Engineering Board,. Washington DC, United States of America: National Academies of Sciences, Engineering, and Medicine.

[5] EULAIR - EUropean Light AIRcraft (2019a), “Fiche Technique”, available at Données Techniques : https://www.eulair.fr/fiche-technique/ (accessed 05 May 2019)

[6] EULAIR - EUropean Light AIRcraft (2019b), “data sheet”, available at Technical Data: http://www.eulair.fr/en/wp-content/uploads/Data-sheet.pdf (accessed 05 May 2019)

[7] EULAIR - EUropean Light AIRcraft (2019c), “mass balance”, available at Technical Data: http://www.eulair.fr/en/wp-content/uploads/Mass-balance.pdf (accessed 05 May 2019)

[8] Isikveren, A.T. (2018), “Kick-off of AVT-RTG-310 HEADSTART”, Meeting No. 1, 19 April 2018, Research Task Group AVT-RTG-310 Hybrid/Electric Aircraft Design and STAndards for Research and Technology (HEADSTART), Applied Vehicle Technology Panel, Science and Technology Organization, NATO.

[9] Isikveren, A.T. (2019), "Fundamentals, Pre-Design Methods and Various Studies of Hybrid/Electric Aeronautical Vehicles", Habilitation à Diriger les Recherches thesis, Institut Supérieur de l'Aéronautique et de l'Espace (SUPAERO-ISAE), 26 June 2019, Toulouse, France.

[10] Isikveren, A.T., Schmidt, M. (2014), "Future Transport Aircraft Ultra-Low Emissions Technology Options", GARS Workshop Air Transport and Climate Change, Worms, Germany.

[11] Meier, O., Scholz, D. (2010), "A Handbook Method for the Estimation of Power Requirements for Electrical De-icing Systems", Deutscher Luft- und Raumfahrtkongress 2010, Hamburg, Germany.

[12] NATO (2009), "NATO UAV Classification Guide".

[13] Python Software Foundation (2019), "python", available at: https://www.python.org/ (accessed 09 February, 2019)

[14] Raymer, D.P. (2012), "Aircraft Design: A Conceptual Approach", American Institute of Aeronautics and Astronautics, Inc., Washington D.C., United States of America.

[15] Riboldi, C.E.D. (2018), "An optimal approach to the preliminary design of small hybrid-electric aircraft", AEGATS.

[16] Torenbeek, E. (1982), Synthesis of Subsonic Airplane Design, Delft University Press, Delft, The Netherlands.

[17] TXT e-solutions (2019), "Pacelab APD", available at: https://www.txtgroup.com/markets/solutions/pacelab-apd/ (accessed 20 February, 2019)

[18] van Blyenburgh, P. (2006), "UAV Systems: Global Review", Avionics 2006 conference, Amsterdam, The Netherlands.

[19] Verstraete D., Palmer, L.L. (2018), "Database of Unmanned Aerial Vehicles", Meeting No. 1, 19 April 2018, Research Task Group AVT-RTG-310 Hybrid/Electric Aircraft Design and STAndards for Research and Technology (HEADSTART), Applied Vehicle Technology Panel, Science and Technology Organization, NATO.

[20] Yezeguelian, A. (2019), "Modelling and Simulation of a Propulsive Hybridisation for a Light Fixed-wing Aircraft", Masters thesis in Aeronautics, Department of Aeronautical and Vehicle Engineering, Kungliga Tekniska Högskolan, Stockholm, March.

[21] Zarati, K., Maalouf, S., Isikveren, A.T. (2017), "Potential of the Bottom Organic Rankine Cycle to Recover Energy on Turboprop Engine Architecture", ISABE-2017-21345, 23rd International Society for Air Breathing Engines (ISABE) Conference, Manchester, United Kingdom.

6 DEFINITIONS, ACRONYMS AND ABBREVIATIONS

ARCH n	Propulsion and Power System architecture candidate number n	HEPPS	Hybrid-Electric Propulsion and Power System
CLB	Climb phase	MALE	Medium Altitude Long Endurance
CROR	Contra-Rotating Open Rotor	MTOW	Maximum Take-Off Weight
CRZ	Cruise phase	OML	Outer Mould Lines

ORC	Organic Rankine Cycle
PMAD	Power Management And Distribution
PPS	Propulsion and Power System
SOC	State Of Charge
TO	Take-Off phase
TOD	Take-Off Distance
TOW	Take-Off Weight
TRL	Technology Readiness Level
TTC	Time-To-Climb
UAV	Unmanned Aerial Vehicle
VAPARE	Variant Autarkic-PARallel-hybrid-electric Eulair drone